DISCRETE AND CONTINUOUS
DYNAMICAL SYSTEMS–SERIES B
Volume **4**, Number **1**, February **2004**

Website: http://AIMsciences.org

pp. **221–240**

BIOLOGICAL STOICHIOMETRY OF TUMOR DYNAMICS: MATHEMATICAL MODELS AND ANALYSIS

Yang Kuang

Department of Mathematics and Statistics
Arizona State University
Tempe, Arizona 85287-1804

John D. Nagy

Department of Biology
Scottsdale Community College
9000 E. Chaparral Road
Scottsdale, AZ 85256-2626

James J. Elser

Department of Biology
Arizona State University
Tempe, AZ 85287-1501

Abstract. Many lines of evidence lead to the conclusion that ribosomes, and therefore phosphorus, are potentially important commodities in cancer cells. Also, the population of cancer cells within a given tumor tends to be highly genetically and physiologically varied. Our objective here is to integrate these elements, namely natural selection driven by competition for resources, especially phosphorus, into mathematical models consisting of delay differential equations. These models track mass of healthy cells within a host organ, mass of parenchyma (cancer) cells of various types and the number of blood vessels within the tumor. In some of these models, we allow possible mechanisms that may reduce tumor phosphorous uptake or allow the total phosphorus in the organ to vary. Mathematical and numerical analyses of these models show that tumor population growth and ultimate size are more sensitive to total phosphorus amount than their growth rates are. In particular, our simulation results show that if an artificial mechanism (treatment) can cut the phosphorus uptake of tumor cells in half, then it may lead to a three quarter reduction in ultimate tumor size, indicating an excellent potential of such a treatment. Also, in general we find that tumors with a relatively high cell death rate are more susceptible to treatments that block phosphorus uptake by tumor cells. Similarly, tumors with a large phosphorus requirement and (or) low cell reproductive rates are also strongly affected by phosphorus limitation.

1. **Introduction.** As a field of study, cancer biology has just begun a "grand synthesis" of sorts. The greatest contributors to this synthesis are the geneticists and cell biologists whose discoveries have uncovered so much of basic cell machinery that at least the broad outlines of how cancer cells develop and act are becoming clear (see reviews by Hahn and Weinberg 2002, Hannahan and Weinberg 2000 and Lundberg and Weinberg 1999). However, newcomers, including evolutionary

2000 *Mathematics Subject Classification.* 34K20, 92C50, 92D25.

Key words and phrases. Biological stoichiometry, tumor model, delay differential equations, qualitative analysis.

biologists and ecologists, are contributing new perspectives that may significantly affect our understanding of the clinical behavior of tumors.

One might wonder what more we need to know if we already understood, say, the details of every biochemical and genetic process occurring within every cancer cell? The problem is that malignant tumors have properties of great clinical significance that are difficult to deduce and explain from first principles of their cell and molecular biology alone. For example, all cancer cells live in an ecological system that requires them to interact with surrounding cells, both healthy and malignant. Studies in cell and molecular biology have shown how some cancers coerce surrounding healthy cells into a servile role in the tumor stroma. However, those same cancer cells must compete with these healthy cells for resources, including oxygen, nutrients and space. The competition does not end there; cancer cells compete against each other and against healthy cells throughout the body for these same resources. Approaches from cell biology will define the basic properties of those relationships, but it will be almost impossible to use cell biology alone to predict the outcomes of these interactions. However, such considerations are dreadfully important clinically. If left to complete its normal course, the competition between tumor and host leads to a generalized wasting syndrome of the host's body called cachexia, which occurs in about half of all cancer patients (Tisdale 1997, Barber *et al.* 1999).

One resource over which cancer and healthy cells may compete is phosphorus. Many lines of evidence suggest that cancer cells upregulate ribosome synthesis, a process that requires large amounts of phosphate (Budde and Grummt 1998, Cairns and White 1998, Zhai and Comai 2000). In addition, certain cancer-related genes, both tumor suppressors (gatekeepers) like $p53$ and oncogenes, including members of the *myc* family, are involved in regulating production of ribosomes (Boon *et al.* 2001, Donahue *et al.* 2001, Greasley *et al.* 2000). Additional studies indicate that cancer cells with larger, more active nucleoli proliferate more rapidly *in vivo* (Derenzini *et al.* 2000a,b). Since the nucleolus is the site of rDNA transcription and the initial stages of ribosome formation, these results highlight ribosome biogenesis as a central process in tumor biology.

Competition for phosphorus or any other resource provided by the host potentially has enormous significance to the clinical course of any malignancy. Cancer cells suffer a characteristic genomic instability that manifests as gross chromosomal abnormality and aneuploidy along with mutations associated with disrupted DNA repair mechanisms (Loeb 1996, Testa 1996). Therefore, the population of cancer cells within a given tumor tends to be highly genetically and physiologically varied (see, for example, Bertuzzi *et al.* 2002). So, we have the elements required for natural selection: a population of genetically varied individuals in a fierce competition for resources. Therefore it is possible that natural selection, in addition to its putative role in determining the incidence of cancer in the first place (Ponder 2001, Simpson 1997), plays an important role in the clinical behavior of cancer.

One obvious example of the power that natural selection has over clinical tumor behavior is tumor cell resistance to chemotherapy or radiation therapy. But even without an "outside" influence like chemotherapy, natural selection probably influences the gross behavior of malignant tumors. For example, in lung cancer, individual tumors typically contain cells characteristic of more than one histological type; in fact, individual cells themselves can possess cytologic features of more than one type of lung cancer (Mabry *et al.* 1996). Therefore, Mabry *et al.* 1996) suggest that histological features of lung cancers change over time, and such changes are

characteristic of tumor progression throughout the tumor's life. One can view this dynamic histology as a result of natural selection acting on various parenchyma cell types as they compete for resources.

Recent work in the fields of ecosystem ecology and life-history evolution has produced a set of ideas and analytical frameworks, "biological stoichiometry" and the "growth rate hypothesis", that we argue have strong relevance for tumor biology. Biological stoichiometry is the study of the balance of energy and multiple chemical elements in biological systems (Sterner and Elser 2002). **The growth rate hypothesis proposes that ecologically significant variations in the relative requirements of an organism for C, N and P are determined by its mass-specific growth rate because of the heavy demand for P-rich ribosomal RNA under rapid growth** (Elser *et al.* 2000). Numerous experimental data show that P-rich animals are unusually sensitive to the P-content of their foods, suffering strong declines in growth and reproduction when consuming food low in P, making them vulnerable to erratic population dynamics and possible extinction in environments that do not supply sufficient P (Sterner and Elser 2002).

The purpose of this paper is to introduce these concepts to cancer biologists, explore the utility of applying these ideas to a model of tumor dynamics, and to describe some potential implications of a stoichiometric view for preventative and therapeutic strategies in cancer. We propose a conceptualization in which tumor and host are seen as a coupled ecological system, each with particular material demands that establish the terms of the interaction and thus affect tumor dynamics. The goal in cancer therapy is to assure that the host (patient) wins in this ecological competition or, at the least, that there is a long-term stable coexistence between the two in which the host maintains an acceptable level of health.

Current therapeutic approaches centered on destroying individual cancer cells or slowing their reproduction, while increasingly successful for many cancers (Brenner 2002), may be inherently limited in their ability to defeat many forms of cancer (Gatenby et al. 2002). But, by applying a stoichiometric perspective to better reflect the multivariate material demands and transactions of the players, health care professionals might be better able to turn the tables of competition in favor of the patient. To do this, we need to understand the functional ecology of the evolving tumor in its co-evolving host habitat.

Our objective here is to integrate these elements, namely the growth rate hypothesis and natural selection driven by competition for phosphorus, into a family of mathematical models. Each tracks mass of healthy cells within a host organ, mass of parenchyma (cancer) cells of various types and the number of blood vessels within the tumor. To be more realistic, these models consist of three or more nonlinear delay differential equations. This continues the trend of using delay differential equations to model life science processes (Kuang 1993, Li *et al.* 2001).

2. Mathematical models of tumor growth with nutrient limitation.

This set of models applies to a single solid tumor growing within a given organ. The organ, like the tumor, is capable of growth, but we typically assume that the organ's initial mass starts near some genetically determined, "healthy" carrying capacity, k_h, and the tumor is initially vascularized but still relatively small (approximately 0.01 kg). In addition, the tumor parenchyma may contain distinct cell types that differ in their nutrient use and growth rates.

Therefore, our dependent variables include the following: x is mass (in kg) of healthy cells within the organ; y_i represents tumor mass (in kg) contributed by

the ith parenchyma cell type; and z expresses mass (in kg) of tumor microvessels. Biologically, z really tracks mass of mature vascular endothelial cells (VECs) within the tumor.

We assume that the total amount of phosphorus within the organ is homeostatically regulated at a fixed value, P (in g). However, phosphorus is distributed into two compartments: extracellular, including blood plasma and interstitial fluid; and intracellular, which contains fraction f (approximately 2/3) of the total fluid within a typical organ (Ganong 1999). Let n represent mean amount of phosphorus (g) in 1 kilogram of healthy cells, including both healthy organ tissue and VECs within the tumor stroma. Similarly, let m be mean amount of phosphorus in 1 kilogram of parenchyma cells. Then

$$P - (nx + my + nz) \equiv P_e$$

is extracellular phosphorus within the organ. A recent report (Chu *et al.* 2002) suggests that normal tissues are about 1% elemental phosphorus (dry weight) and tumor tissues are often over 2% (dry weight).

2.1. **Homogeneous tumor.** We first build the model for the special case of a tumor with only one parenchyma cell type. In this model, reproduction of both healthy and tumor cells is a function of amount of extracellular phosphorus. In a phosphorus-rich environment, healthy cells and tumor cells can proliferate at maximum per capita rates a and b, respectively. However, if the extracellular phosphorus concentration drops below a threshold value, then growth rates of both healthy and tumor cells are impaired. This consideration is adopted in Andersen (1997) and Loladze *et al.* (2000).

For healthy cells, if extracellular phosphorus concentration P_e/fk_h is less than n, the mean phosphorus content in a kilogram of healthy cells, then per capita growth rate without crowding effects becomes

$$a\frac{P_e}{fnk_h}.$$

A similar set of relationships governs blood vessel dynamics and tumor cell growth, except in the case of tumor cells, the growth rate decreases whenever concentration of extracellular phosphorus drops below m. When that happens, maximal tumor growth rate becomes $b\dfrac{P_e}{fmk_h}$.

Reproduction of tumor cells is further modified by blood supply. Specifically, tumor proliferation rate slows whenever vascularization drops below a certain threshold. In particular, whenever $g(z-\alpha y)/y < 1$, then the maximum proliferation rate of tumor cells becomes $g(z-\alpha y)/y$, where α represents the mass of cancer cells that one unit of blood vessels can just barely maintain, and g measures sensitivity of tumor tissue to lack of blood.

In this model we assume that cancer cells suffer a constant per capita mortality, d_y. In addition, the tumor's growth rate decelerates as it approaches its "carrying capacity," k_t. Once it reaches that size, proliferation and mortality balance each other. The value of k_t is determined by the physiological status of the host and in human breast cancer, for example, is approximately 1.0 to 2.3 kg (Spratt *et al.* 1993).

Similarly, we assume that healthy cells die at constant per capita rate d_x. But, since the tumor competes with healthy tissue for resources, especially blood, the organ "feels" the tumor. Therefore, the growth rate of healthy tissue decelerates as

the mass of both the healthy and tumor tissue approaches k_h. A similar situation does not apply to the tumor. The tumor growth rate is only modified by the relationship between tumor mass and tumor carrying capacity, k_t; mass of healthy tissue has no effect on the tumor.

Blood vessel dynamics are much simpler. First, we assume that new microvessels arise from activated VEC precursor cells within the tumor stroma at per capita rate c if there is no phosphorus limitation. We also assume there is a time delay τ between activation of vascular precursor cells and construction of functional vessels. This delay represents the time it takes for VEC precursor cells to respond to angiogenic growth factors, divide, degrade their basement membranes, migrate to the site of growth and mature into working endothelium (Ji *et al.* 1998).

At this moment, it is not clear to us whether or not construction of blood vessel is phosphorus limiting. If not, then the recruitment term is simply $cy(t-\tau)$. If phosphorus is limiting, then the recruitment term becomes $\frac{cP_e}{fnk_h}y(t-\tau)$. For realistic parameters, simulation results suggest that the qualitative dynamics of the model are essentially unchanged whether phosphorus is limiting or not (figure 9). However, if blood vessel construction is not phosphorus limited, then the tumor reaches its ultimate size a couple of days sooner than it would if the construction of blood vessel is phosphorus limited. The differences in the ultimate organ and tumor sizes are negligible. For this reason, we will conduct our simulation work on models assuming that blood vessel construction is phosphorus limited but conduct our mathematical analysis on the model assuming that it is NOT phosphorus limited.

Some evidence suggests that the vascular network within tumors is constantly being remodeled (Columbo *et al.* 1996). To reflect this observation, we assume that mature vessels die at a constant rate d_z.

These considerations lead to the following model:

$$\begin{aligned}
\frac{dx}{dt} &= x\left(a\min\left(1,\frac{P_e)}{fnk_h}\right) - d_x - (a-d_x)\frac{x+y+z}{k_h}\right),\\
\frac{dy}{dt} &= y\left(b\min\left(1,\beta\frac{P_e}{fmk_h}\right)\min(1,L) - d_y - (b-d_y)\frac{y+z}{k_t}\right),\\
\frac{dz}{dt} &= c\min\left(1,\frac{P_e}{fnk_h}\right)y(t-\tau) - d_z z,\\
L &= \frac{g(z-\alpha y)}{y}.
\end{aligned} \tag{2.1}$$

We have introduced an extra parameter, β, into model (2.1) for the purpose of exploring the dynamic effects of artificially limiting phosphorus uptake by cancer cells, by inhibiting membrane transport of phosphate, for instance. When there is no such therapeutic intervention, $\beta = 1$; when therapy is instituted, $\beta < 1$. Also note that when neither blood supply nor phosphorus are limiting, cancer cell dynamics become logistic.

2.2. **Heterogeneous tumor.** In actual malignant tumors one often finds a variety cell types competing for various resources. In the context of model (2.1), these resources include phosphorus, space and blood supply. In this paper we focus on competition for the first two resources; competition for blood supply will be dealt with at another time.

Although actual tumors can contain many parenchyma cell types, we simplify the system to only two competing varieties, the masses of which are represented

by y_1 and y_2. We assume that parenchyma cell types can differ from each other in only two ways: they may have different intrinsic birth and death rates, b_1 and b_2, d_1 and d_2, respectively; and they may differ in their efficiency of phosphorus use, meaning that in general $m_1 \neq m_2$, where m_i is the mean phosphorus content of the i-th cell type.

These assumptions lead to the following extension of model (2.1) to include two competing cell types:

$$\begin{aligned}
\frac{dx}{dt} &= x\left(a\min\left(1,\frac{P_e}{fnk_h}\right) - d_x - (a-d_x)\frac{x+y_1+y_2+z}{k_h}\right),\\
\frac{dy_1}{dt} &= y_1\left(b_1\min\left(1,\frac{\beta_1 P_e}{fm_1k_h}\right)\min(1,L) - d_1 - (b_1-d_1)\frac{y_1+y_2+z}{k_t}\right),\\
\frac{dy_2}{dt} &= y_2\left(b_2\min\left(1,\frac{\beta_2 P_e}{fm_2k_h}\right)\min(1,L) - d_2 - (b_2-d_2)\frac{y_1+y_2+z}{k_t}\right),\\
\frac{dz}{dt} &= c\min\left(1,\frac{P_e}{fnk_h}\right)(y_1(t-\tau)+y_2(t-\tau)) - d_z z,\\
L &= g\frac{z-\alpha(y_1+y_2)}{y_1+y_2},
\end{aligned} \tag{2.2}$$

where P_e becomes $P - nx - m_1y_1 - m_2y_2 - nz$. Again, we introduced parameters β_1 and β_2 in the tumor growth equations to measure the effects of artificially regulating phosphorus uptake by parenchyma cells. Note that model (2.2) reduces to model (2.1) when $y_2(0) = 0$, with the obvious modifications of subscripts.

In a different context, recent work of Loladze *et al.* (2000) suggests that stoichiometric constraints promote coexistence among competing species. One goal of our analysis of model (2.2) will be to determine if such a statement can be made in the case of heterogeneous tumor growth. Our simulation results indicate that the answer is negative.

2.3. **Heterogeneous tumor model with dietary regulation.** In this final extension of the model we introduce a time-varying organ phosphorus content. First, we assume that a constant proportion, γ, of dead cell material, particularly phosphorus, is removed per unit time from the organ by the blood. Also, we assume that phosphorus ingested with food is brought to the organ at rate r (g/day). Then in the setting of a heterogeneous tumor (model 2.2), these assumptions yield an equation that tracks the total phosphorus in the organ:

$$\begin{aligned}
\frac{dP}{dt} = \; & r - \gamma\Bigg(n(d_x x + d_z z) + (a-d_x)nx\frac{x+y_1+y_2+z}{k_h}\\
& + \textstyle\sum_{i=1}^{2} m_i d_i y_i + \dfrac{y_1+y_2+z}{k_t}\displaystyle\sum_{i=1}^{2} m_i(b_i-d_i)\Bigg).
\end{aligned}$$

Each negative term represents phosphorus liberated by dying cells, both healthy and cancerous, that is subsequently washed out of the tumor by the blood.

Together with the assumptions of model (2.2), we obtain the following model of a heterogeneous tumor with varying total phosphorus:

$$\begin{aligned}
\frac{dx}{dt} &= x\left(a\min\left(1,\frac{P_e}{fnk_h}\right)-d_x-(a-d_x)\frac{x+y_1+y_2+z}{k_h}\right),\\
\frac{dy_1}{dt} &= y_1\left(b_1\min\left(1,\frac{P_e}{fm_1k_h}\right)\min(1,L)-d_1-(b_1-d_1)\frac{y_1+y_2+z}{k_t}\right),\\
\frac{dy_2}{dt} &= y_2\left(b_2\min\left(1,\frac{P_e}{fm_2k_h}\right)\min(1,L)-d_2-(b_2-d_2)\frac{y_1+y_2+z}{k_t}\right),\\
\frac{dz}{dt} &= c\min\left(1,\frac{P_e}{fnk_h}\right)(y_1(t-\tau)+y_2(t-\tau))-d_zz,\\
\frac{dP}{dt} &= r-\gamma\Bigg(n(d_xx+d_zz)+(a-d_x)nx\frac{x+y_1+y_2+z}{k_h}+\sum_{i=1}^{2}m_id_iy_i+\\
&\qquad \frac{y_1+y_2+z}{k_t}\sum_{i=1}^{2}m_i(b_i-d_i)\Bigg),\\
L &= g\frac{z-\alpha(y_1+y_2)}{y_1+y_2},
\end{aligned} \tag{2.3}$$

where P_e now becomes $P(t)-nx-m_1y_1-m_2y_2-nz$. For a tumor-free patient it is reasonable to assume that the organ size sits at its carrying capacity, and supply and depletion of plasma phosphorus is balanced through food intake. In such scenario, $r=\gamma ank_h$. For a healthy person of 70 kg in weight, we estimate his/her daily consumption of nutritious solid food at about 1.5 kg/day. If we assume the phosphorus content of food is about 1.4 g for each kilogram, then daily dietary phosphorus intake is about 2.1 g (Kapur 2000). For a 10 kg organ, its share of phosphorus is about 0.3 g/day, assuming a homogeneous distribution throughout the body. These considerations put $\gamma=0.001$ when $a=3$ and $n=k_h=10$ at tumor-free equilibrium (see Figure 8).

A potential treatment strategy may emerge if we know how different values of r change the dynamic outcomes of tumor growth in model (2.3).

3. **Simulation analysis of the mathematical models.** Mathematically, each of the many minimum functions in models (2.1)-(2.3) divides the dynamics into two categories. Therefore, for the simplest model (2.1), there are eight possible dynamical scenarios. It is both challenging and time-consuming to gain a complete analytical understanding of all possible variations of these three high-dimensional, nonlinear delay differential equation models. However, realistic parameter values often naturally restrict or eliminate some possibilities, thereby rendering the analyses of most mathematically possible dynamical scenarios unnecessary. It is thus logical to perform some simulation work with biologically meaningful parameters and initial values prior to any serious analytical treatment of our models. Indeed, as we shall see, only one dynamical scenario of our models is biologically plausible and important enough to merit careful mathematical study.

We assume that patients vary in size and that organ and tumor carrying capacities vary in the same direction. As a result, it is easy to observe that our models are invariant with proper scaling of all variables and parameters. With this property in mind, we perform our simulation on only one generic patient – a person with a body mass of about 70 kg and about 700 g of total body phosphorous (Kapur 2000). For concreteness we assume the tumor arises in the lung, which has a mass of about 15

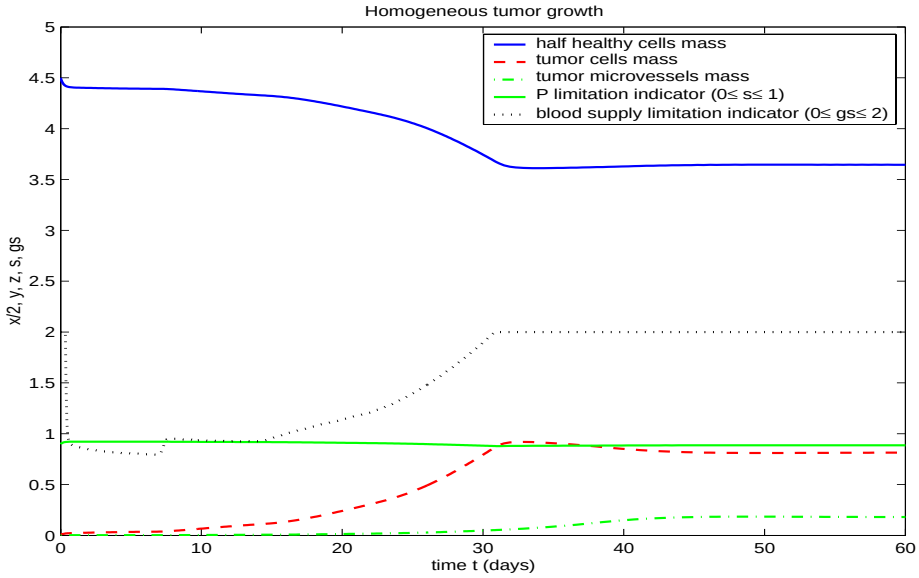

FIGURE 1. A solution for model (2.1) with $a = 3, m = 20, n = 10, k_h = 10, k_t = 3, f = 0.6667, P = 150, \alpha = .05, b = 6, \tau = 7, c = .05, d_x = d_y = 1, d_z = 0.2, g = 100$ and $(x(0), y(0), z(0)) = (9, 0.01, 0.001)$. Here we assume no treatment blocking phosphorus uptake by tumor cells ($\beta = 1$). Notice that phosphorus limits the growth of both healthy and tumor cells (the phosphorus limitation indicator $s < 1$.)

kg including extracellular fluid (about 6 kg). Furthermore, if we assume that the phosphorous is evenly distributed throughout our patient's body, then the lung's share of phosphorous is about 150 g. We further assume that the initial tumor size is large enough for detection (about 0.01 kg) and therefore is already vascularized.

We begin by investigating models (2.1) and (2.2), in which organ phosphorus content is held constant. Our extensive simulation work shows that in these models tumor growth and ultimate size are much more sensitive to total amount of phosphorus in the lung than tumor growth rate is (compare figures 1, 2 and 3). When phosphorus is the most limiting factor for tumor growth, as opposed to blood supply, ultimate tumor size is roughly proportional to total amount of phosphorus in the lung. Our simulation results for the model (2.3), where total body phosphorus is allowed to vary, are consistent with these findings (figure 8). In all simulation figures we plot both the P limitation indicator (denoted by $s = \min\left(1, \frac{P_e}{fnk_h}\right)$) and the blood supply limitation indicator (denoted by $gs = \min\left(1, \frac{g(z - \alpha y)}{y}\right)$) to help visualize when these are indeed limiting healthy and tumor cell growth.

Simulation also indicates that the time delay τ tends to affect how long it takes a tumor to reach a given size much more dramatically than changes in organ phosphorus content ($P(t)$) or sensitivity of tumor cells to lack of blood (g) (compare figure 1 and figure 4). Note that simulation results of the first τ days are transitional

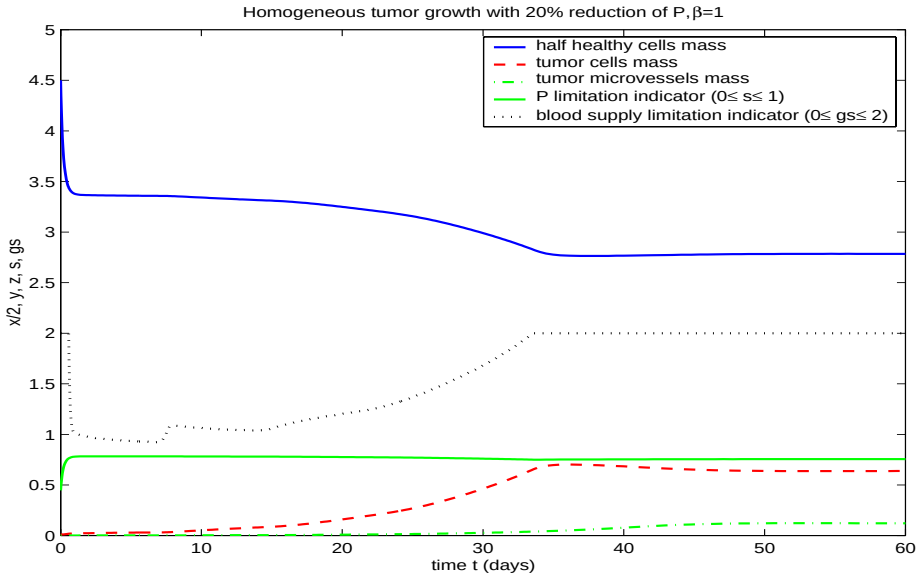

FIGURE 2. A solution for model (2.1). All parameters and initial values are identical to that of figure 1, except that we have lowered P by 20% to 120. Notice that the ultimate tumor size is reduced slightly more than 20% (from about 0.96 kg to 0.73 kg). It should be mentioned here that the organ suffers a similar percent reduction in weight.

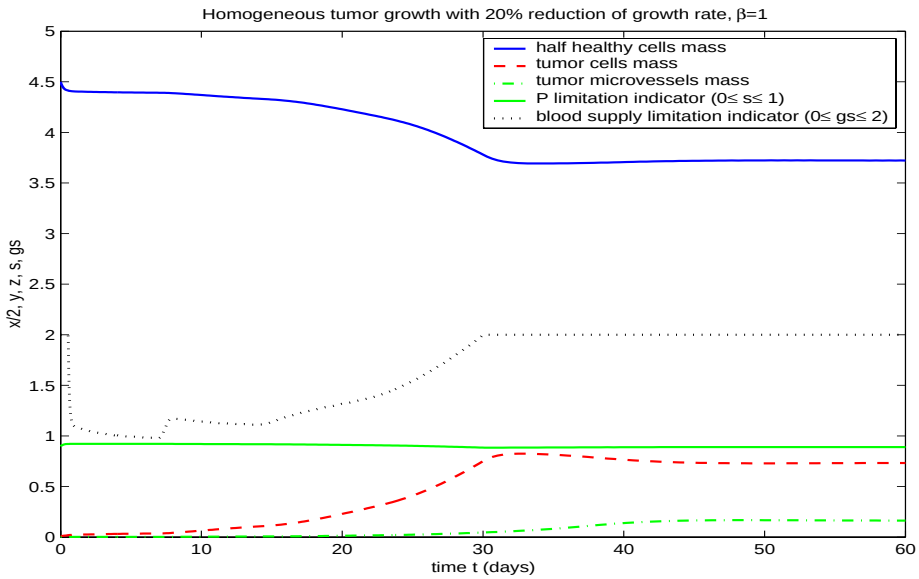

FIGURE 3. A solution for model (2.1). All parameters and initial values are identical to that of figure 1, except we have lowered tumor birth rate b by 20% to 4.8. The ultimate tumor size is reduced by about 10% (from about 0.96 kg to 0.86 kg). As to be expected, the organ enjoys a small percent increase in weight.

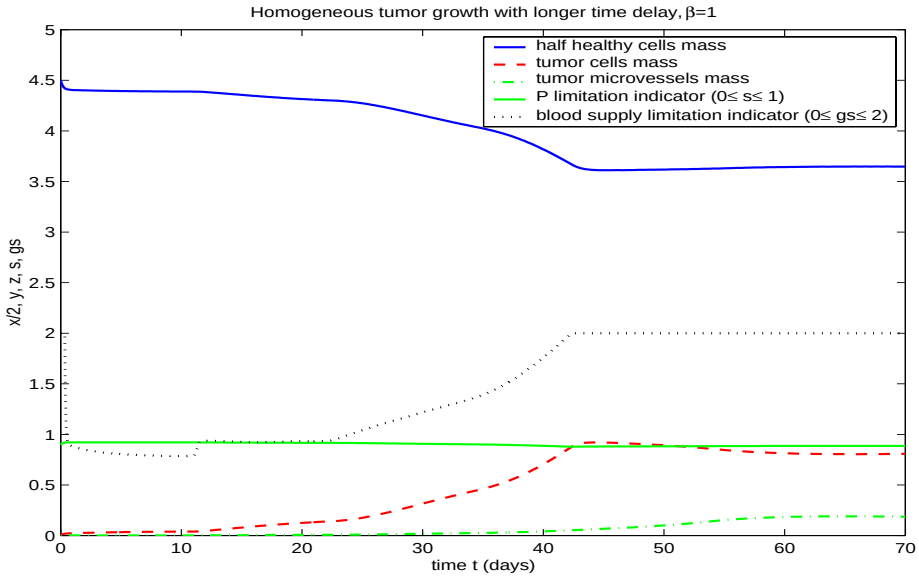

FIGURE 4. A solution for model (2.1). All parameters and initial values are identical to that of figure 1, except we have increased the time delay τ from 7 to 11. The ultimate tumor and organ sizes are unchanged, but the approach to equilibrium is postponed from about day 32 to day 44.

and may contain artifacts caused by the initial conditions, a commonly observed phenomena in numerical solutions of delay differential models.

When the tumor contains two parenchyma cell types, then we often observe that the less malignant type, characterized by a lower phosphorus requirement and hence lower proliferation and death rates, tends to quickly dominate the tumor (figure 7). The same conclusion holds true when several tumor cell species coexist in the tumor.

Phosphate supplementation is a common supportive therapy for oncology patients suffering hypophosphatemia. However, such supplementation must be carefully monitored because of complications associated with the opposite condition, hyperphosphatemia, most notably hypocalcemia (Warrell 2001). At first sight it may appear that our models argue for a universal restriction of phosphate in a cancer patient's diet; indeed, phosphate supplementation may simply be feeding the tumor (compare figures 1 and 2). We explored this issue more deeply with model (2.3). Our results suggest that dietary phosphorus restriction alone is unlikely to benefit our patient. While it is true that, in the context of model (2.3), dietary restriction of phosphorus can reduce tumor growth and ultimate size, both ultimate tumor size and organ size change in the same direction – in fact, almost proportionally (figure 2). Therefore, restricting phosphorus damages the healthy organ as much as it does the tumor.

Given this result, we might search for ways to reduce tumor phosphorus uptake without affecting phosphorus availability to healthy cells. How beneficial would such a treatment be? We can address this question by activating such a possible mechanism in models (2.1) and (2.2) by assuming that β, β_1 and β_2 are less than

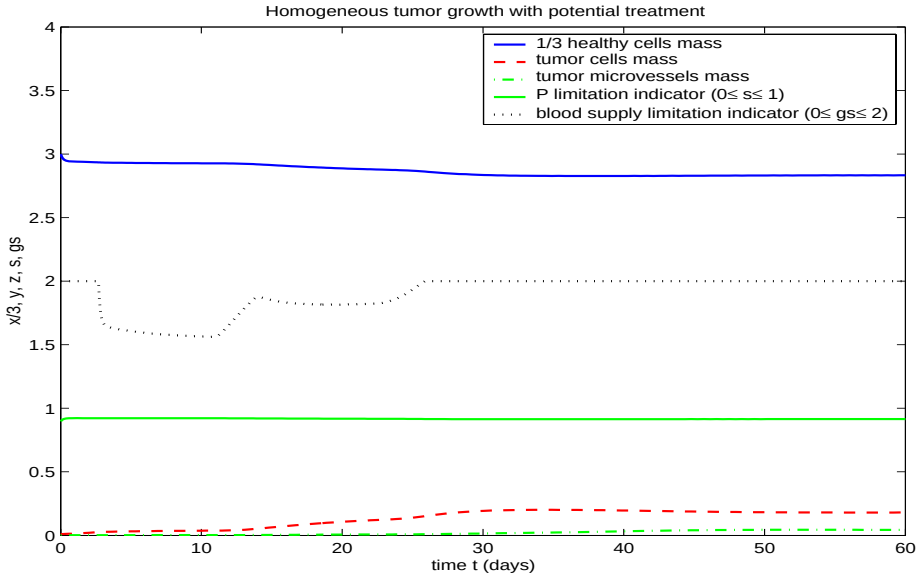

FIGURE 5. A solution for model (2.1). All parameters and initial values are identical to that of figure 1, except we have selectively blocked tumor cell uptake of phosphorus by half ($\beta = 0.5$). The ultimate tumor size is now less than a quarter of that in figure 1. In addition, the organ maintains its healthy size. This result suggests an excellent potential for such a treatment strategy.

1. When playing out such a scenario in model (2.1) by setting $\beta = 0.5$, we reduce ultimate tumor size by about 75% (figure 5) while maintaining the organ at a healthy size. Therefore, selectively limiting phosphorus to tumor cells may prevent the tumor from reaching a lethal size. However, if phosphorus is not limiting, then such mechanism may not be useful, as confirmed by our simulation when we increase P from 150 to 250 in model (2.1) (figure 6).

An interesting phenomenon in all these models is that ultimate tumor size is insensitive to its predetermined carrying capacity. A tumor's ultimate size depends mostly on phosphorus supply. For a large range of values, the parameter g does not affect the tumor size but does change the time it takes for a tumor to reach certain size. An indirect observation through simulation work of model (2.3) suggests that only about 0.1% of the P released from the dead tumor cells is flushed out by the blood. In other words, almost all phosphorus stays in the organ. This raises the possibility of excessive P accumulating in the organ after any treatment that kills a large amount of tumor cells, such as some drug treatments modelled in Jackson, 2002. This result, therefore, explains a well-described phenomenon called "tumor lysis syndrome" in which plasma phosphorus concentration reaches toxic levels after tumors have been treated with chemotherapy.

4. **Mathematical analysis of the models.** For realistic parameter values and initial conditions, the ultimate outcome of all three models is the same: solutions tend to a positive steady state where phosphorus limits both healthy and tumor cell growth. One nonintuitive phenomenon is that at this steady state, tumor growth is

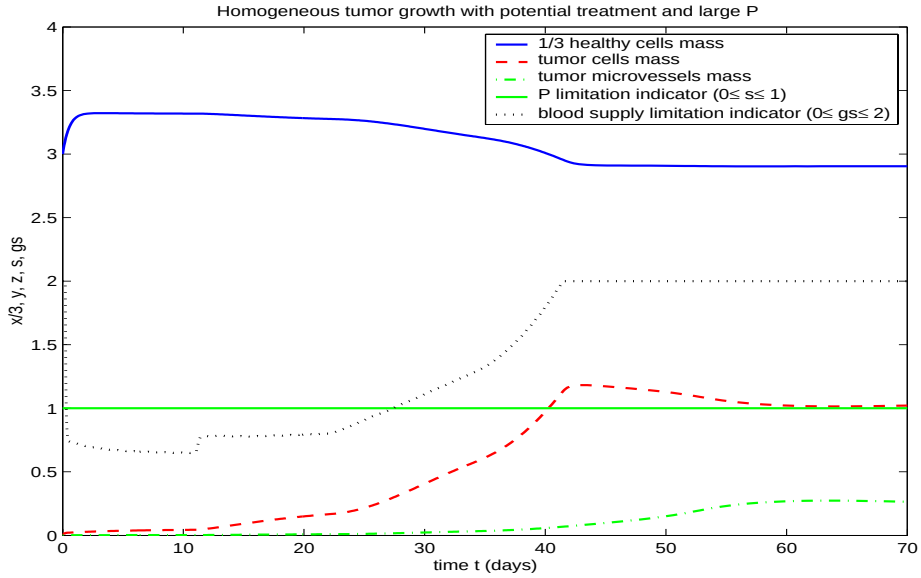

FIGURE 6. A solution for model (2.1). All parameters and initial values are identical to that of figure 5, except that we have substantially increased the total body phosphorus to $P = 250$ from 150. This change makes phosphorus no longer limiting (phosphorus limitation indicator $s = 1$). In this situation, the tumor still grows to a large size even when the tumor's phosphorus uptake is halved. This result cautions that selectively inhibiting tumor cell phosphorus uptake, if possible, must be accompanied by dietary control to be effective.

no longer limited by its blood vessel infrastructure. For this reason, we shall study in detail the properties of this important steady state.

A comparison of figures 1 and 7 indicates that when the tumor is viewed as a single entity, models (2.1) and (2.2) essentially generate the same dynamics. Moreover, varying the supply of phosphorus continuously seems to create no new dynamical behavior to speak of (figure 8). Hence, we will limit our mathematical analysis to homogeneous tumor growth.

Although the dynamics of model (2.1) with realistic parameters appears to be simple – solutions tend to the unique positive steady state E – it defies any in-depth mathematical treatment, including finding the expression and stability properties of its positive steady state. However, a realistic simplification presents itself because, as we noted in section 2, the qualitative dynamics of the model are essentially unchanged whether phosphorus limits blood vessel construction (figure 9). Therefore, in this section we will assume that

(A1): The construction of blood vessels is NOT limited by phosphorus supply.

With (A1), model (2.1) becomes the following simplified model:

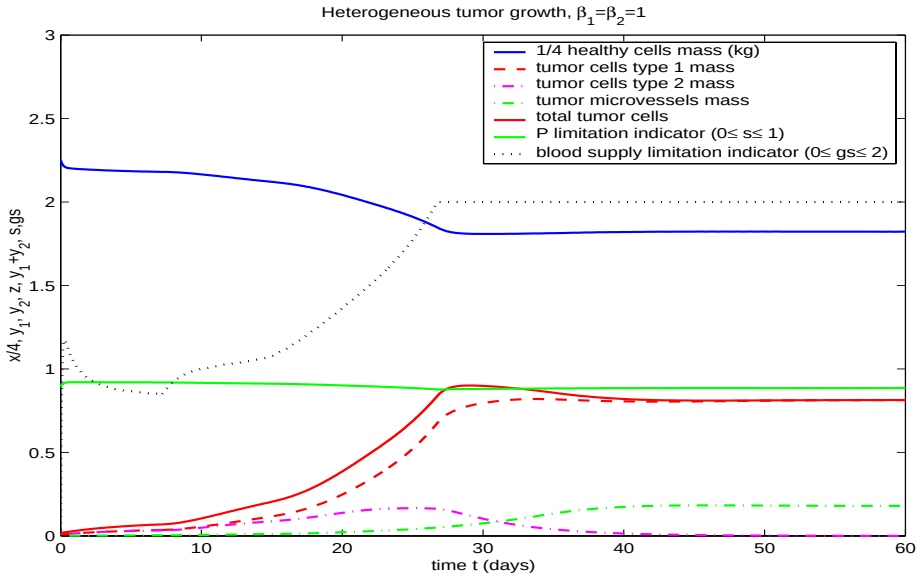

FIGURE 7. A solution for model (2.2) with $a = 3, m_1 = 20, m_2 = 22, n = 10, k_h = 10, k_t = 3, f = 0.6667, P = 150, \alpha = .05, b_1 = 6, b_2 = 6.6, \tau = 7, c = .05, d_x = 1, d_z = 0.2, d_1 = 1, d_2 = 1, g = 100$ and $(x(0), y_1(0), y_2(0), z(0)) = (9, 0.01, 0.01, 0.001)$. This is a typical example showing that tumor cell types with lower phosphorous requirements (in this case y_1) wins.

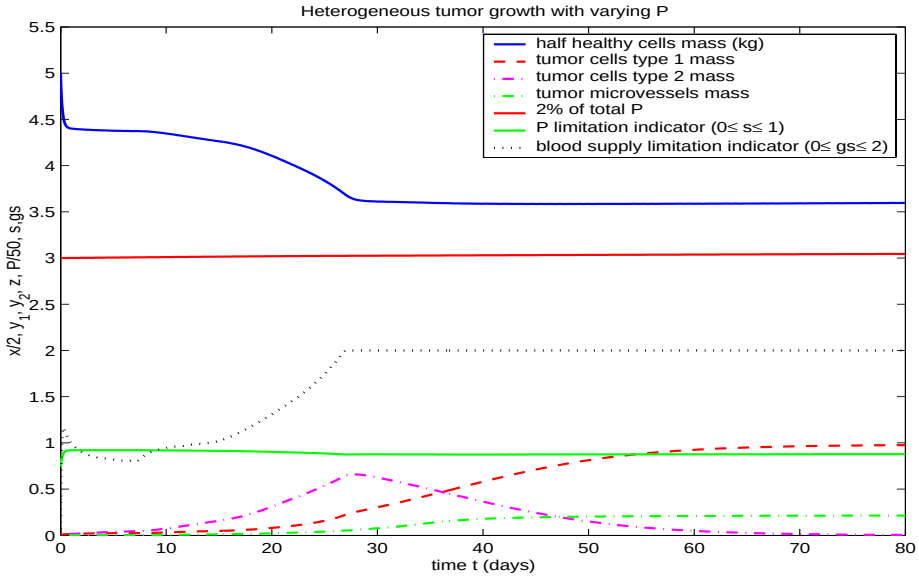

FIGURE 8. A solution for model (2.3). In this situation, if no tumor cells were present, the organ would remain at its steady state, $x = 10$ kg.

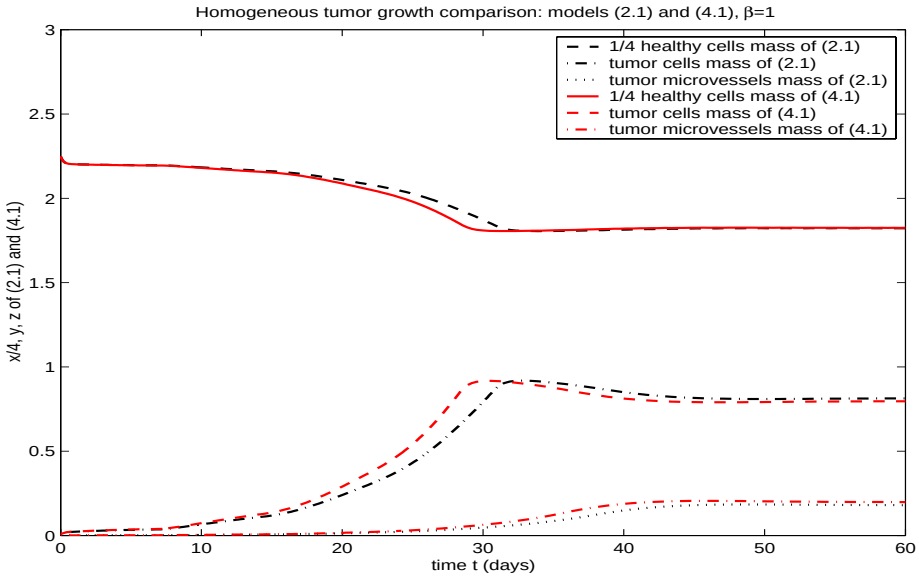

FIGURE 9. Solutions of models (2.1) and (4.1), with $a = 3, m = 20, n = 10, k_h = 10, k_t = 3, f = 0.6667, P = 150, \alpha = .05, b = 6, \tau = 7, c = .05, d_x = d_y = 1, d_z = 0.2, g = 100$ and $(x(0), y(0), z(0)) = (9, 0.01, 0.001)$.

$$\begin{aligned}
\frac{dx}{dt} &= x\left(a\min\left(1, \frac{P_e}{fnk_h}\right) - d_x - (a - d_x)\frac{x+y+z}{k_h}\right),\\
\frac{dy}{dt} &= y\left(b\min\left(1, \beta\frac{P_e}{fmk_h}\right)\min(1, L) - d_y - (b - d_y)\frac{y+z}{k_t}\right),\\
\frac{dz}{dt} &= cy(t-\tau) - d_z z,\\
L &= \frac{g(z-\alpha y)}{y}.
\end{aligned} \tag{4.1}$$

Support for the validity of A1 comes from the fact that the difference between ultimate sizes of tumors described by models (2.1) and (4.1) are negligible. For example, in one run a tumor described by model (2.1) approached 0.8138 kg, whereas in model (4.1) with the same parameters it settled on a mass of 0.7963 kg.

Our main concern in this section is the stability of the positive steady state E^* of (4.1). Our analysis is simplified by the following observation: in both models (2.1) and (4,1), at this steady state E^*, $\dfrac{P_e}{fnk_h} < 1$ and $L > 1$ (figure 10). Hence we assume further that

(A2): For model (4.1), $\dfrac{P_e}{fnk_h} < 1$ and $L > 1$ at E^*.

Clearly (A2) implies that $\dfrac{\beta P_e}{fmk_h} < 1$. With this additional assumption, we obtain the following explicit expression of $E^* = (x^*, y^*, z^*)$:

$$\begin{aligned} x^* &= \frac{k_h}{a-d_x}\left[\frac{an}{\beta bm}\left(d_y+(b-d_y)\frac{y^*+z^*}{k_t}\right)-d_x\right]-y^*-z^*, \\ y^* &= d_z k_t N/D, \\ z^* &= ck_t N/D. \end{aligned} \tag{4.2}$$

where

$$N = aPb\beta - d_xPb\beta - d_yk_hma - afmk_hd_y + b\beta nd_xk_h + fd_xmk_hd_y$$

and

$$\begin{aligned} D = {} & -fd_xd_zmk_hb - ad_zfmk_hd_y - fd_xcmk_hb - acfmk_hd_y - ad_zmk_hd_y + \\ & ad_zmk_hb + acfmk_hb + ad_zmk_tb\beta + fd_xd_zmk_hd_y - d_xd_zmk_tb\beta + ad_zfmk_hb \\ & -k_tb\beta d_zna + k_tb\beta d_znd_x + fd_xcmk_hd_y + acmk_hb - acmk_hd_y. \end{aligned}$$

Notice that $y^* = 0$ if and only if

$$N = aPb\beta - d_xPb\beta - d_yk_hma - afmk_hd_y + b\beta nd_xk_h + fd_xmk_hd_y = 0.$$

This yields a threshold value for β, which we denote by β^*,

$$\beta^* = \frac{d_yk_hma + afmk_hd_y - fd_xmk_hd_y}{(a-d_x)Pb + bnd_xk_h} = \frac{m}{b}k_hd_y\frac{a(f+1)-fd_x}{(a-d_x)P+nd_xk_h}.$$

When the parameters assume values as in Figure 1, that is $a = 3, m = 20, n = 10, k_h = 10, f = 0.6667, P = 150, b = 6, d_x = 1, d_y = 1$, we have $\beta = 0.3611166667$, as confirmed by simulation (Figure 11). Since $1-\beta$ measures the proportion of the tumor's P uptake blocked by the treatment, we see that the higher the tumor cell death rate, the smaller the proportion of tumor cell P uptake needs to be blocked to eliminate the tumor. A similar statement holds true for the tumor's P content requirement (m), whereas the opposite is true for the tumor's birth rate (b).

In order to study stability aspects of the steady state E^* of (4.1), we need the following lemma, the proof of which follows directly from that of Theorem 6.5.2 (page 227) in Kuang, 1993.

LEMMA 4.1. *Assume that the parameters in the following system are positive, and* $x^* > 0, y^* > 0, z^* > 0$*:*

$$\begin{aligned} \frac{dx}{dt} &= -x(A_1(x-x^*)+A_2(y-y^*)+A_3(z-z^*)), \\ \frac{dy}{dt} &= -y(B_1(x-x^*)+B_2(y-y^*)+B_3(z-z^*)), \\ \frac{dz}{dt} &= -(-c(y(t-\tau)-y^*)+d_z(z-z^*)). \end{aligned} \tag{4.3}$$

If there are positive constants c_1, c_2 *such that*
1): $d_z > c/c_2$,
2): $B_2/c_2 > B_3 + B_1/c_1$,
3): $A_1/c_1 > A_1 + A_2/c_2$
then the steady state $E^* = (x^*, y^*, z^*)$ *is globally asymptotically stable.*

Near the steady state E^*, model (4.1) can be rewritten in the form of system (4.3) with

$$A_1 = \frac{1}{k_h}\left(\frac{a}{f}+a-d_x\right) = A_3, \qquad A_2 = \frac{1}{k_h}\left(\frac{am}{fn}+a-d_x\right) \tag{4.4}$$

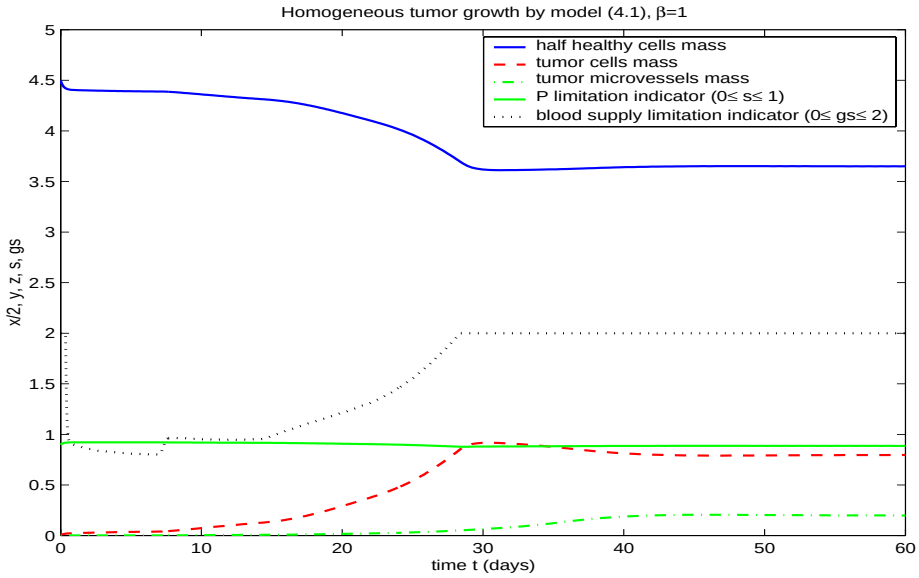

FIGURE 10. A solution for model (4.1) with $a = 3, m = 20, n = 10, k_h = 10, k_t = 3, f = 0.6667, P = 150, \alpha = .05, b = 6, \tau = 7, c = .05, d_x = d_y = 1, d_z = 0.2, g = 100$ and $(x(0), y(0), z(0)) = (9, 0.01, 0.001)$. Here we assume no treatment blocking phosphorus uptake by tumor cells ($\beta = 1$) and the construction of blood vessel is NOT phosphorus limited. Notice that $\dfrac{P_e}{fnk_h} < 1$ and $L > 1$ at E^* for model (4.1).

and

$$B_1 = \frac{b\beta n}{fk_h m}, \qquad B_2 = \frac{b\beta}{fk_h} + \frac{b - d_y}{k_t}, \qquad B_3 = \frac{b\beta n}{fk_h m} + \frac{b - d_y}{k_t}. \tag{4.5}$$

For $a = 3, m = 20, n = 10, k_h = 10, f = 0.6667, P = 150, b = 6, d_x = 1, d_y = 1, \beta = 1$, we can chose $c_1 = 0.5$ and $c_2 = 0.2$ to satisfy conditions 1) through 3) in Lemma 4.1. **In other words, we have shown that for this set of parameters, the positive steady state E^* of model (4.1) is locally asymptotically stable**. However, simulation suggests that it is actually globally asymptotically stable. So, this mathematical question remains open.

As we increase P in model (4.1), the condition $\dfrac{P_e}{fnk_h} < 1$ may be violated, and the positive steady state may become the positive solution of

$$\begin{aligned} x^* + y^* + z^* &= k_h, \\ B_1 x^* + B_2 y^* + B_3 z^* &= \frac{b\beta P}{fmk_h} - d_y, \\ cy^* - d_z z^* &= 0, \end{aligned} \tag{4.6}$$

where $B_i, i = 1, 2, 3$ are given by (4.5). In this case, we have

$$y^* = \frac{(b\beta P)/(fmk_h) - d_y - B_1 k_h}{B_2 - B_1 + (B_3 - B_1)c/d_z}.$$

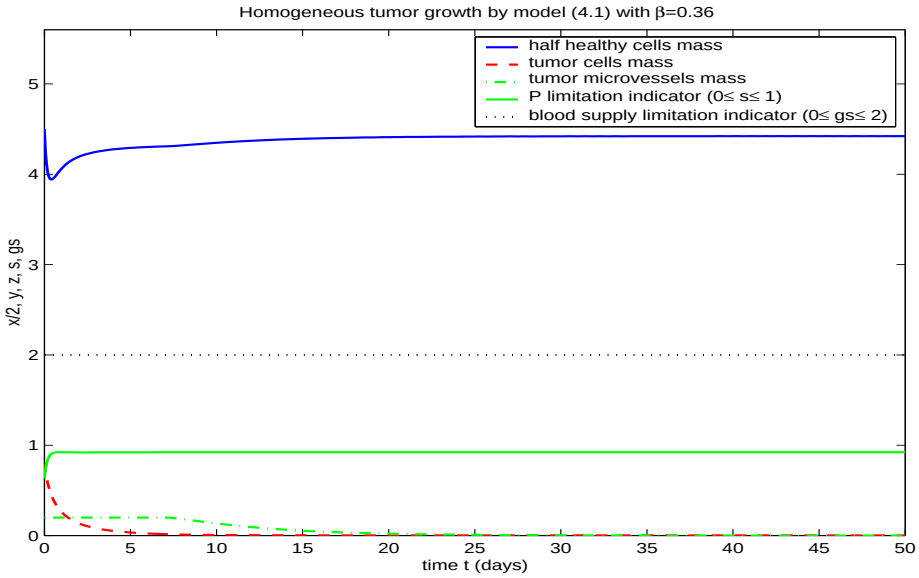

FIGURE 11. A solution for model (4.1) with $\beta = 0.36, a = 3, m = 20, n = 10, k_h = 10, k_t = 3, f = 0.6667, P = 150, \alpha = .05, b = 6, \tau = 7, c = .05, d_x = d_y = 1, d_z = 0.2, g = 100$ and $(x(0), y(0), z(0)) = (9, 0.8, 0.2)$. Here we assume a treatment yielding a 64% reduction in phosphorus uptake by tumor cells, and the construction of blood vessel is NOT phosphorus limited.

Using Lemma 4.1, we can also show that this steady state is locally asymptotically stable.

A sufficiently large increase in P will lead to a scenario in which $\dfrac{\beta P_e}{fmk_h} > 1$. For example, when $a = 3, m = 20, n = 10, k_h = 10, f = 0.6667, P = 150, b = 6, d_x = 1, d_y = 1, \beta = 1$, we need $P > 257.34$. In such a case, the positive steady state is simply $E^* = (k_h - k_t, d_z k_t/(c + d_z), ck_t/(c + d_z))$, which again by Lemma 4.1, is locally asymptotically stable.

We summarize the above statements into the following theorem.

THEOREM 4.1. *Assume that in model (4.1) there is a unique positive steady state $E^* = (x^*, y^*, z^*)$. Assume further that there are positive constants c_1, c_2 such that*
1): $d_z > c/c_2$,
2): $B_2/c_2 > B_3 + B_1/c_1$,
3): $A_1/c_1 > A_1 + A_2/c_2$
where A_1, A_2, B_1, B_2, B_3 are given by (4.4) and (4.5). Then the steady state $E^* = (x^*, y^*, z^*)$ is locally asymptotically stable.

In our simulation study, we assume that both normal and tumor cell birth rate is proportional to per unit phosphorous content (that is $ma = nb$); suppose also that the cell death rate is the same for both normal and tumor cells. If in addition, there is no treatment – that is $\beta = 1$ – then we have the following

Special Case: $ma = nb, d_x = d_y, \beta = 1$.

In this special case, we have

$$\begin{aligned} y^* &= \frac{aP - fnk_h d_x}{fn(a-d_x)(\rho+1+\sigma) + a(n\rho+m+n\sigma)} \\ &= \frac{bP - fmk_h d_y}{fm(a-d_y)(\rho+1+\sigma) + b(n\rho+m+n\sigma)}, \end{aligned}$$

where

$$\sigma = \frac{c}{d_z}, \qquad \rho = \left(\frac{b-d_y}{k_t} - \frac{a-d_x}{k_h}\right)\frac{k_h(1+\sigma)}{a-d_x}.$$

Notice that σ represents the units of tumor biomass supported by a unit of vascular endothelial cells (VECs) within the tumor body. This expression of tumor steady state size shows that P plays a clear and prominent role in determining its value. We observe that the tumor dies out if one can increase the tumor's death rate or the tumor's P requirement, or lower the tumor's birth rate to certain threshold levels.

5. **Discussion.** Our model should be viewed as an attempt to understand the growth dynamics of a single vascularized solid tumor growing within the confines of a organ, such as a primary lung or breast tumor. Our model stresses competition within the environment provided by that organ: healthy and tumor cells competing for both space and essential but limiting nutrients, although here we consider only carbon and phosphorous. The form of our models consists of three or more nonlinear delay differential equations. If applied clinically, such models may be useful in predicting the time courses of various aspects of tumor dynamics, such as tumor size and growth rate at a given future date. Therefore, they may give rise to useful tools that oncologists can use to help decide the proper course of treatment for specific patients. However, we caution that the models presented here were not designed for direct clinical application. Much more specific information and rigorous comparisons between model results and actual tumors is required before they are applied to treatment decisions in any way.

In the convoluted path leading us to these models, we formulated over a dozen plausible alternatives and performed extensive simulations on all of them. Surprisingly, all demonstrate similar growth dynamics. In particular, all strongly suggest that stoichiometric constraints are important model features. Specifically, we observe that phosphorus availability plays a key role in tumor growth and size, more so than either birth or death rates. Without such stoichiometric constraints, tumors will invariably follow the simple logistic equation and quickly grow to their carrying capacities.

The most noteworthy insight gained through this modelling exercise is that within the tumor entity, slower-growing tumor cell types, which utilize less phosphorus because their ribosome production demands are not as great, will dominate the tumor over the time. This competitive exclusion pressure always threatens to push faster-growing cell types to extinction, which in turn may provide the evolutionary impetus for these more aggressive tumor cells to metastasize. This result may explain why metastatic tumor cells typically differ from those that dominate the primary tumor. One should explore how this evolutionary insight might be exploited clinically.

One obvious recommendation suggested by this research is to look for ways to selectively reduce the rate of phosphorus uptake by tumor cells. The advantage of such a treatment is that it may dramatically reduce ultimate tumor size while maintaining the organ at a healthy size. This result could be accomplished by

applying drugs capable of selectively blocking phosphorus uptake by tumor cells. Alternatively, one could use a nutritionally worthless inhibitor that competes with phosphate for the binding site on membrane phosphate transporters. This strategy is particularly intriguing since it would tend to avoid the toxic effect of excessive phosphorus liberated from dead tumor cells, a situation that causes, in part, "tumor lysis syndrome," a well known phenomenon that results from destruction of tumor cells during chemotherapy (Warrell 2001). Unfortunately, since little is known about phosphorus transport by cells outside the kidney tubules or small intestine, more specific suggestions regarding what agents would be most useful are not possible.

A second plausible treatment suggested by this research is to implant into the tumor less malignant or benign tumor cells, or simply healthy cells if possible, that require less phosphorus and thus are likely to out-compete the original tumor cells. Alternatively, one can try to genetically manipulate existing tumor cells to generate less malignant or benign tumor cells that will do the same thing.

REFERENCES

[1] Andersen, T. (1997): *Pelagic nutrient cycles: herbivores as sources and sinks.* Springer-Verlag, New York, NY.

[2] Barber, M.D., J.A. Ross and K.C. Fearon (1999): Cancer cachexia. *Surg. Oncol.*, **8**, 133-41.

[3] Bertuzzi, A., M. Faretta, A. Gandolfi, C. Sinisgalli, G. Starace, G. Valoti and P. Ubezio (2002): Kinetic heterogeneity of an experimental tumour revealed by BrdUrd incorporation and mathematical modeling. *Bull. Math. Biol.*, **64**, 355-84.

[4] Boon, K., H.N. Caron, R. van Asperen, L. Valentijn, R.-C. Hermus, P. van Sluis, I. Roobeek, I. Weis, P.A. Voute, M. Schwab and R. Versteeg (2001): N-myc enhances the expression of a large set of genes functioning in ribosome biogenesis and proteins synthesis. *EMBO*, **20**, 1383-93.

[5] Brenner, H. (2002): Long-term survival rates of cancer patients achieved by the end of the 20th century: a period analysis. *Lancet*, **360**, 1131-35.

[6] Budde, A. and I. Grummt (1998): p53 represses ribosomal gene transcription. *Oncogene*, **19**, 1119-24.

[7] Cairns, C.A. and R.J. White (1998): p53 is a general repressor of RNA polymerase III transcription. *EMBO*, **17**, 3112-23.

[8] Chu, T.Y., K.S. Hwang, M.H. Yu, H.S. Lee, H.C. Lai and J.Y. Liu (2002): A research-based tumor tissue bank of gyneocologic oncology: characteristics of nucleic acids extracted from normal and tumor tissues from different sites, *Int. J. Gynecol. cancer*, **12**, 171-6.

[9] Columbo, M.P., L. Lombardi, C. Melani, M. Parenza, C. Baroni, L. Ruco and A. Stoppacciaro (1996): Hypoxic tumor cell death and modulation of endothelial adhesion molecules in the regression of granulocyte colony-stimulating factor-transduced tumors. *Am. J. Pathol.*, **148**, 473-83.

[10] Derenzini, M., D. Trere, A. Pession, M. Govoni, V. Sirri and P. Chieco (2000): Nucleolar size indicates the rapidity of cell proliferation in cancer tissues. *J. Pathol.*, **191**, 181-6.

[11] Derenzini, M., D. Trere, A. Pession, L. Montanaro, V. Sirri and R.L. Ochs (2000): Nucleolar function and size in cancer cells. *Am. J. Pathol.*, **152**, 1291-7.

[12] Donahue, R.J., M. Razmara, J.B. Hoek and R.B. Knudsen (2001): Direct influence of the p53 tumor suppressor on mitochondrial biogenesis and function. *FASEB*, **15**, 635-44.

[13] Elser, J.J., R.W. Sterner, E. Gorokhova, W.F. Fagan, T.A. Markow, J.B. Cotner, J.F. Harrison, S.E. Hobbie, G.M. Odell and L.J. Weider (2000): Biological Stoiciometry from genes to ecosystems. *Ecology Lett.*, **3**, 540-50.

[14] Ganong, W.F. (1999): *Review of medical physiology.* 19th ed. Appleton and Lange, Stamford, Connecticut.

[15] Gatenby, R.A., P.K. Maini, E.T. Gawlinski (2002): Analysis of tumor as an inverse problem provides a novel theoretical framework for understanding tumor biology and therapy. *Appl. Math. Lett.*, **15**, 339-45.

[16] Greasley, P.J., C. Bonnard and B. Amati (2000): Myc induces the nucleolin and BN51 genes: possible implications in ribosome biogenesis. *Nuc. Acids Res.*, **28**, 446-53.

[17] Hannahan, D. and R.A. Weinberg (2000): The hallmarks of cancer. *Cell*, **100**, 57-70.
[18] Hahn, W.C. and R.A. Weinberg (2002): Modelling the molecular circuitry of cancer. *Nature Rev.*, **2**, 331-41.
[19] Jackson, T.L. (2002): Vascular tumor growth and treatment: consequences of polyclonality, competition and dynamic vascular support. *J. Math. Biol.*, **44**, 201-26.
[20] Ji, W.-R., F.J. Castellino, Y. Chang, M.E. Deford and H. Gray (1998): Characterization of kringle domains of angiostatin as antagonists of endothelial cell migration, and important process in angiogenesis. *FASEB*, **12**, 1731-8.
[21] Jordan, P. and M. Carmo-Fonseca (1998): Cisplatin inhibits synthesis of ribosomal RNA *in vivo*. *Nuc. Acids Res.*, **26**, 2831-6.
[22] Kapur, S. (2000): A medical hypothesis: phosphorus balance and prostate cancer. *Cancer Investigation*, **18**, 664-9.
[23] Kuang, Y. (1993): *Delay differential equations with applications in population dynamics.* New York, Academic Press.
[24] Li, J., Y. Kuang and B. Li (2001): Analyses of IVGTT glucose-insulin interaction models with time delay, *Discrete Contin. Dynam. Systems, B*, **1**, 103-24.
[25] Loeb, L. A. (1996): Many mutations in cancer. *Cancer Surveys*, **28**, 329-42.
[26] Loladze, I., Y. Kuang and J.J. Elser (2000): Stoichiometry in producer-grazer systems: Linking energy flow with element cycling. *Bull. Math. Biol.*, **62**, 1137-62.
[27] Lundberg, A.S. and R.A. Weinberg (1999): Control of the cell cycle and apoptosis. *European J. Cancer*, **35**, 1886-94.
[28] Mabry, M., B. Nelkin and S. Baylin (1996): Evolutionary model of lung cancer. *In:* Lung cancer: principles and practice. H.I. Pass, J.B. Mitchell, D.H. Johnson and A.T. Turrisi [eds.]. Lippencott-Raven, Philadelphia, PA 133-42.
[29] Ponder, B.A.J. (2001): Cancer genetics. *Nature*, **411**, 336-41.
[30] Simpson, A.J.G. (1997): The natural somatic mutation frequency and human carcinogenesis. *Adv. Cancer Res.*, **71**, 209-40.
[31] Spratt, J.A., D. von Fournier, J.S. Spratt and E.E. Weber (1993): Decelerating growth and human breast cancer. *Cancer*, **71**, 2013-9.
[32] Sterner, R.W. and J.J. Elser (2002): *Ecological Stoichiometry.* Princeton University, Princeton, NJ.
[33] Testa, J.R. (1996): Chromosome alterations in human lung cancer. *In:* Lung cancer: principles and practice. H. I. Pass, J. B. Mitchell, D. H. Johnson and Andrew T. Turrisi [eds.]. Lippencott-Raven, Philadelphia, PA 55-71.
[34] Tisdale, M.J. (1997): Biology of cachexia. *J. Nat. Cancer Instit.*, **89**, 1763-73.
[35] Warrell, R.P. (2001): Metabolic emergencies. *In:* Cancer: principles and practice of oncology. V. T. DeVita, Jr., S. Hellman and S. A. Rosenberg [eds.]. Lippincott, Williams and Wilkens, Philadelphia, PA 2633-45.
[36] Zhai, W. and L. Comai (2000): Repression of RNA polymerase I transcription by the tumor suppressor p53. *Mol. Cell. Biol.*, **20**, 5930-8.

Received October 2002; revised May 2003.

E-mail address: kuang@asu.edu